

Particle linear theory on a self-gravitating perturbed cubic Bravais lattice

B. Marcos*

*“E. Fermi” Center, Via Panisperna 89 A, Compendio del Viminale, I-00184 Rome, Italy,
‡ ISC-CNR, Via dei Taurini 19, I-00185 Rome, Italy.*

Abstract

Discreteness effects are a source of uncontrolled systematic errors of N-body simulations, which are used to compute the evolution of a self-gravitating fluid. We have already developed the so-called “Particle Linear Theory” (PLT), which describes the evolution of the position of self-gravitating particles located on a perturbed simple cubic lattice. It is the discrete analogue of the well-known (Lagrangian) linear theory of a self-gravitating fluid. Comparing both theories permits to quantify precisely discreteness effects in the linear regime. It is useful to develop the PLT also for other perturbed lattices because they represent different discretizations of the same continuous system. In this paper we detail how to implement the PLT for perturbed cubic Bravais lattices (simple, body and face-centered) in a cubic simulation box. As an application, we will study the discreteness effects — in the linear regime — of N-body simulations for which initial conditions have been set-up using these different lattices.

PACS numbers: 98.80.-k, 05.70.-a, 02.50.-r, 05.40.-a

I. INTRODUCTION

One of the most important open problems in cosmology is the formation of the large scale structure. The key process involved is the gravitational clustering of dark matter, which is still not well understood. It is considered to be well described as a self-gravitating fluid for a wide range of scales (e.g. [1]). The complexity of these fluid equations (coupled with gravity) makes impossible to compute an analytical solution. There are therefore two common approaches to attack the problem: (i) a perturbative expansion in the density contrast $\delta(\mathbf{r}) = \rho(\mathbf{r})/\rho_0 - 1$ (where $\rho(\mathbf{r})$ is the local density and ρ_0 its space average), valid only at early times (or for scales in which the density contrast averaged over such scales is smaller than one) and (ii) N-body simulation, in which the fluid is discretized into particles (N-bodies) and then the evolution of the system computed applying simple gravity.

N-body simulations are used to compute the evolution in the highly non-linear regime. A basic problem of this method is that there is no theory on the discreteness effects due to the use of a finite number N of particles (e.g. [2, 3, 4, 5, 6, 7]). Generally, tests varying N shows a “convergence” of the simulations. However, it is difficult to infer how well this convergence has been achieved because of the lack of framework to refer to. For example, it is not known the dependence of the discreteness error with N . If the convergence is slow, numerical tests can indeed appear to converge when actually convergence has not been achieved (see e.g. [7, 8]).

In [9] and subsequently [10, 11, 12] we have started to develop a program to precisely fill this gap. We have

developed a framework which allows us to calculate the evolution — in the linear regime — of a system of self-interacting particles. This is the discrete counterpart of the well-known *Fluid Linear Theory* (hereafter FLT), and we called it *Particle Linear Theory* (hereafter PLT). We have shown that the fluid limit of the PLT is well defined and indeed it is the FLT. We have shown also how to quantify, in an essentially analytic way, the discreteness effects, with arbitrarily large precision. Moreover, disposing of analytical results permits to evaluate the discreteness effects in the limit of infinite realizations. It avoids, in the computation of statistical quantities, the use of any statistical estimator and thus its subsequent and problematic noise. One of our conclusions was that, for the set-up of the initial conditions (IC), the body centered cubic lattice could be a better choice than the simple cubic (sc) one, because it might produce less discreteness effects. We will see in this paper that it is indeed the case in this context of linear theory.

Moreover, another important motivation of this paper is the study of the discreteness effects in the *non-perturbative* regime. In the forthcoming paper [13] we sample the *same* continuous field using different lattices and then evolve them using N-body simulations. The differences between the result of these simulations give an estimate of the lower bound of the discreteness effects in the *non-perturbative regime*. Because these differences are small — typically of order of a few percent in the power spectrum for times and scales relevant to cosmological simulations —, an implementation of the PLT for these lattices is an essential tool to check that these differences are actually discreteness effects and not numerical errors, finite-size effects, estimator-related errors, etc.

In this paper we present the PLT method applied to any cubic Bravais lattice, i.e., to a simple cubic (sc), body-centered (bcc) and face-centered (fcc) lattices. In the first section we give an summary of the PLT. Further

*Electronic address: Bruno.Marcos@roma1.infn.it

details can be found in [10]. In the following section, we explicitly give the details of the PLT for a sc, bcc and fcc lattices. We use Fast Fourier Transform techniques, in a *cubic box*, which is a-priori non trivial. In the last section, we present some applications of the method, comparing discreteness effects using a perturbed sc, bcc or fcc lattice to set-up the IC. It is a generalization to a bcc and fcc lattices of the work presented in [12].

II. LINEARIZATION OF GRAVITY ON A PERTURBED LATTICE

In this section we present a summary of the general method we have developed in [10, 11] to calculate the evolution of self-gravitating particles perturbed off a perfect lattice.

Let us consider a parallelepiped of volume V with N lattice sites, which are generated combining linearly the three primitive lattice vectors \mathbf{a}_1 , \mathbf{a}_2 and \mathbf{a}_3 :

$$\mathbf{R} = \mathbf{R}(n_1, n_2, n_3) = \ell(n_1\mathbf{a}_1 + n_2\mathbf{a}_2 + n_3\mathbf{a}_3), \quad (1)$$

where

$$n_i \in [0, N_i - 1] \cap \mathbb{Z} \quad (2)$$

and ℓ is the typical ‘‘lattice spacing’’¹ (we have chosen \mathbf{a}_i to be dimensionless). The total number of particles in the system is $N = N_1N_2N_3$ and the box a parallelepiped with sides $\mathbf{A} = \{\mathbf{A}_1, \mathbf{A}_2, \mathbf{A}_3\}$, where $\mathbf{A}_i = N_i\mathbf{a}_i$.

We perform a displacement of the particles about their lattice position \mathbf{R} and we write their new position $\mathbf{r}(t)$ as:

$$\mathbf{r}(t) = \mathbf{R} + \mathbf{u}(\mathbf{R}, t), \quad (3)$$

which will evolve under the effect of gravity and where $\mathbf{u}(\mathbf{R}, t)$ is a *displacement field* evaluated at the lattice positions.

A. Definition and linearization of the gravitational force

In order to have a translationally invariant system² we take periodic boundary conditions. We use the *method of replicas* to compute the gravitational force. It consists in calculating the force not only considering the particles in the box of volume V but also all its *images*, i.e., an infinite number of copies of the system. This is a standard scheme in cosmological N-body simulations to evaluate the force (see e.g. [14]). For a well defined gravitational

force in the infinite volume limit, it is necessary to introduce a neutralizing background which, in the context of cosmology, is naturally introduced as a consequence of the expansion (see e.g. [1]).

The gravitational force is linearized by expanding in Taylor series at linear order in the variable $\mathbf{u}(\mathbf{R}, t)$ about the lattice position \mathbf{R} (for more details see e.g. [10]). It is convenient to use of the *dynamical matrix* $\mathcal{D}(\mathbf{R})$ to express the linearized force:

$$\mathbf{F}(\mathbf{r}) = \sum_{\mathbf{R}'} \mathcal{D}(\mathbf{R} - \mathbf{R}')\mathbf{u}(\mathbf{R}'). \quad (4)$$

The expression of the dynamical matrix for a generic interaction potential $v(r)$ is [10]:

$$\mathcal{D}_{\mu\nu}(\mathbf{R} \neq \mathbf{0}) = \partial_\mu \partial_\nu w(\mathbf{R}) \quad (5a)$$

$$\mathcal{D}_{\mu\nu}(\mathbf{R} = \mathbf{0}) = - \sum_{\mathbf{R}' \neq \mathbf{0}} \partial_\mu \partial_\nu w(\mathbf{R}') \quad (5b)$$

where

$$\partial_\mu \partial_\nu w(\mathbf{r}_0) = \left[\frac{\partial^2 w(\mathbf{r})}{\partial r_\mu \partial r_\nu} \right]_{\mathbf{r}=\mathbf{r}_0} \quad (6)$$

and $w(\mathbf{r})$ is the periodic function defined as

$$w(\mathbf{r}) = \sum_{\mathbf{n}} v(\mathbf{r} + \mathbf{n} \cdot \mathbf{A}), \quad (7)$$

i.e., the potential due to a single particle and all its copies. For the gravity force, we have $v(\mathbf{r}) = -Gm/r$ and Eq. (7) is implicitly understood to be regularized by the addition of a uniform negative background. However, the sum (7) is numerically slowly convergent (it is necessary to sum over a huge number of replicas). To speed-up the computation we use the standard Ewald method, which consists in dividing the sum in a short range part and a long range one introducing a damping function \mathcal{C} :

$$\begin{aligned} w(\mathbf{r}) &= \sum_{\mathbf{n}} v(\mathbf{r} + \mathbf{n} \cdot \mathbf{A}) \mathcal{C}(|\mathbf{r} + \mathbf{n} \cdot \mathbf{A}|, \alpha) \\ &+ \sum_{\mathbf{n}} v(\mathbf{r} + \mathbf{n} \cdot \mathbf{A}) [1 - \mathcal{C}(|\mathbf{r} + \mathbf{n} \cdot \mathbf{A}|, \alpha)], \end{aligned} \quad (8)$$

where α is a damping parameter from which the result is independent. A common choice for a $1/r$ potential is

$$\mathcal{C}(|\mathbf{r}|, \alpha) = \text{erfc}(\alpha|\mathbf{r}|). \quad (9)$$

The expression for the function w is then:

$$w(\mathbf{r}) = w^{(r)}(\mathbf{r}) + w^{(k)}(\mathbf{r}) \quad (10)$$

and

$$w^{(r)}(\mathbf{r}) = -Gm \sum_{\mathbf{n}} \frac{1}{|\mathbf{r} + \mathbf{n} \cdot \mathbf{A}|} \text{erfc}(\alpha|\mathbf{r} + \mathbf{n} \cdot \mathbf{A}|), \quad (11a)$$

$$w^{(k)}(\mathbf{r}) = -Gm \frac{4\pi}{V_B} \sum_{\mathbf{k} \neq \mathbf{0}} \frac{1}{|\mathbf{k}|^2} \exp\left(-\frac{|\mathbf{k}|^2}{4\alpha^2}\right) \cos[\mathbf{k} \cdot \mathbf{r}]. \quad (11b)$$

¹ For a sc lattice ℓ is the actual lattice spacing while this is not true in the bcc and fcc case, because all the lattice sites are not at the same distance each one from another.

² This is not to have any privileged point in the system.

The Fourier vectors \mathbf{k} are generated combining linearly the (dimensionless) primitive vectors in reciprocal space \mathbf{b}_i

$$\mathbf{k}\ell = m_1 \frac{\mathbf{b}_1}{N_1} + m_2 \frac{\mathbf{b}_2}{N_2} + m_3 \frac{\mathbf{b}_3}{N_3} \quad (12)$$

where m_i are integers and

$$\mathbf{a}_i \cdot \mathbf{b}_j = 2\pi\delta_{ij} \quad (13)$$

(δ_{ij} is the Kronecker delta). We define the *Nyquist frequency* as

$$k_N = \frac{\pi}{\ell}. \quad (14)$$

It is simple to show (e.g [10]) that the term $\mathbf{k} = \mathbf{0}$ is not included in the sum (11b) due to the presence of the neutralizing background (or the space expansion in the cosmological context). An explicit expression of the dynamical matrix is given in App. A.

B. Dynamical equations

For simplicity we will consider a matter-dominated universe with zero cosmological constant (Einstein-deSitter, hereafter EdS)³. This is a very good approximation for the currently most favored Λ CDM cosmological model for the times in which PLT is a good approximation (i.e. before shell-crossing), considering the typical red-shifts in which the simulations are started. The evolution of the displacement field $\mathbf{u}(\mathbf{R}, t)$ is given by the equation

$$\ddot{\mathbf{u}}(\mathbf{R}, t) = -2\frac{\dot{a}}{a}\dot{\mathbf{u}}(\mathbf{R}, t) + \frac{1}{a^3} \sum_{\mathbf{R}'}^N \mathcal{D}(\mathbf{R} - \mathbf{R}')\mathbf{u}(\mathbf{R}', t), \quad (15)$$

where $a(t)$ is the scale factor and the (double) dots mean (double) derivative with respect to time. From Bloch theorem it is possible to diagonalize Eq. (15) in real space using the following combination of plane waves:

$$\mathbf{u}(\mathbf{R}, t) = \frac{1}{N} \sum_{\mathbf{k}} \tilde{\mathbf{u}}(\mathbf{k}, t) e^{i\mathbf{k} \cdot \mathbf{R}}, \quad (16)$$

where the sum is restricted to the *first Brillouin zone* (hereafter FBZ), i.e., by the set of the N vectors \mathbf{k}^4 with smaller modulus. These symmetrically lie around $\mathbf{k} = \mathbf{0}$ ⁵.

³ For a static non-expanding universe see [10].

⁴ It is simple to show (e.g. [15]) that a periodic lattice with N particles has N associated independent vectors \mathbf{k} .

⁵ The FBZ is not in general symmetric about $\mathbf{k} = \mathbf{0}$ but this is the case for a *cubic* Bravais lattice because of the symmetries of the lattice.

We denote $\tilde{\mathbf{u}}(\mathbf{k}, t)$ as the Fourier transform (hereafter FT) on the lattice of $\mathbf{u}(\mathbf{R}, t)$

$$\tilde{\mathbf{u}}(\mathbf{k}, t) = \sum_{\mathbf{R}} \mathbf{u}(\mathbf{R}, t) e^{-i\mathbf{k} \cdot \mathbf{R}}, \quad (17)$$

where the sum is restricted to the simulation box (i.e. without considering the replicas). Using Eqs. (15) and (16) we obtain the 3×3 eigenvalue problem

$$\ddot{\tilde{\mathbf{u}}}(\mathbf{k}, t) = \tilde{\mathcal{D}}(\mathbf{k})\tilde{\mathbf{u}}(\mathbf{k}, t), \quad (18)$$

where $\tilde{\mathcal{D}}(\mathbf{k})$ is defined analogously to $\tilde{\mathbf{u}}(\mathbf{k}, t)$. We can easily diagonalize (numerically) Eq. (18), obtaining for each \mathbf{k} the eigenvalue equation

$$\tilde{\mathcal{D}}(\mathbf{k})\hat{\mathbf{e}}_n(\mathbf{k}) = 4\pi G\rho_0 \varepsilon(\mathbf{k})\hat{\mathbf{e}}_n(\mathbf{k}), \quad (19)$$

where ρ_0 is the average mass density $\rho_0 = n/V$ and $\varepsilon(\mathbf{k})$ the normalized eigenvalues of the dynamical matrix $\tilde{\mathcal{D}}(\mathbf{k})$. We can decompose each mode $\tilde{\mathbf{u}}(\mathbf{k}, t)$ in the basis $\{\hat{\mathbf{e}}_n(\mathbf{k}), n = 1, 2, 3\}$ as

$$\tilde{\mathbf{u}}(\mathbf{k}, t) = \sum_{n=1}^3 \hat{\mathbf{e}}_n(\mathbf{k}) f_n(\mathbf{k}, t). \quad (20)$$

Using Eqs. (18), (19) and (20) we get the following equation for the coefficients $f_n(\mathbf{k}, t)$:

$$\ddot{f}_n(\mathbf{k}, t) + 2\frac{\dot{a}}{a}\dot{f}_n(\mathbf{k}, t) = \frac{4\pi G\rho_0 \varepsilon(\mathbf{k})}{a^3} f_n(\mathbf{k}, t). \quad (21)$$

Depending on the sign of $\varepsilon(\mathbf{k})$, we obtain two classes of solutions $U_n(\mathbf{k}, t)$ and $V_n(\mathbf{k}, t)$, which are given in App. B.

C. Evolution of the power spectrum

Usually, we are not interested in the position of each particle but in some global statistical quantities. In this paper, we will focus on the power spectrum (hereafter PS), defined as

$$P(\mathbf{k}) = \lim_{V \rightarrow \infty} \frac{\langle \delta\tilde{\rho}(\mathbf{k})\delta\tilde{\rho}^*(\mathbf{k}) \rangle}{V}, \quad (22)$$

where $\delta\tilde{\rho}(\mathbf{k})$ is the FT of the density contrast $\delta\rho(\mathbf{r}) = \rho(\mathbf{r}) - \rho_0$ (we assume statistical homogeneity). It is possible to show that for a small value of the displacement $|\mathbf{u}(\mathbf{R}, t)| \ll \ell$, the PS of a perturbed lattice can be written as [9, 16]

$$P(\mathbf{k}, t) \approx k_\mu k_\nu \tilde{g}_{\mu\nu}(\mathbf{k}, t), \quad (23)$$

where

$$\tilde{g}_{\mu\nu}(\mathbf{k}) = \lim_{V \rightarrow \infty} \frac{\langle \tilde{u}_\mu(\mathbf{k})\tilde{u}_\nu^*(\mathbf{k}) \rangle}{V}. \quad (24)$$

Setting-up the IC at $t = t_0$ in the canonical way using the Zeldovich approximation is equivalent to set (e.g. [9])

$$\tilde{g}_{\mu\nu}(\mathbf{k}, t_0) = \hat{\mathbf{k}}_\mu \hat{\mathbf{k}}_\nu \tilde{g}(\mathbf{k}, t_0). \quad (25)$$

Using Eqs. (B8), (B9), (23) and (25) we get:

$$P(\mathbf{k}, t) \approx A_P^2(\mathbf{k}, t) P(\mathbf{k}, t_0), \quad (26)$$

where

$$A_P(\mathbf{k}, t) = \sum_{\mu, \nu} \hat{\mathbf{k}}_\mu \hat{\mathbf{k}}_\nu \mathcal{A}_{\mu\nu}(\mathbf{k}, t) \quad (27)$$

and (for an EdS universe) [10]

$$\mathcal{A}_{\mu\nu}(\mathbf{k}, t) = \sum_{n=1}^3 \left[U_n(\mathbf{k}, t) + \frac{2}{3t_0} V_n(\mathbf{k}, t) \right] (\hat{\mathbf{e}}_n)_\mu (\hat{\mathbf{e}}_n)_\nu. \quad (28)$$

III. DIAGONALIZATION OF THE DYNAMICAL MATRIX

In this section we describe step-by-step how to diagonalize the dynamical matrix.

A. Generation of the real space lattice

In general, N-body simulations are performed in a *cubic* box, using a perturbed lattice as initial conditions. Therefore, to fill the simulation box in an uniform way, the number of particles cannot be arbitrary. In the case of a sc lattice, the number of points should be $N = N_{sc}^3$ (with N_{sc} an integer), for a bcc one $N = (N_{bcc}/2)^3$ and for an fcc one $N = (N_{fcc}/4)^3$ (where N_{bcc} and N_{fcc} are also integers).

Note that the real space vectors \mathbf{R} , generated using Eq. (1), lie, in general, in a *parallelepiped* box, with sides $\{\mathbf{A}_1, \mathbf{A}_2, \mathbf{A}_3\}$. Note that it is necessary to generate the real space vectors in this way [i.e. using Eq. (1) and (2)] in order to use the technique of Fast Fourier Transform (FFT) as we will see in section III C. We have therefore to translate the \mathbf{R} vectors into a cube using a operation which leaves unchanged the dynamics of the system. It is simple to show that the equation of motion (15) is invariant under the transformation

$$\mathbf{R} \longrightarrow \mathbf{R} + \sum_{i=1}^3 n'_i \mathbf{A}_i, \quad (29)$$

(where n'_i are integers). We can, then, choose three primitive lattice vectors $\{\mathbf{a}_i, i = 1, 2, 3\}$ and the number of particles N_i associated with each primitive lattice vector (compatible with the total number of particles) which, using Eq. (29), translate all the lattice sites into a cube. This is not trivial and does not work for any combination of primitive lattice vectors and number of particles

	\mathbf{a}_1	\mathbf{a}_2	\mathbf{a}_3
sc	[1, 0, 0]	[0, 1, 0]	[0, 0, 1]
bcc	[1, 0, 0]	[0, 1, 0]	$\frac{1}{2}$ [1, 1, 1]
fcc	$\frac{1}{2}$ [0, 1, 1]	$\frac{1}{2}$ [1, 0, 1]	[0, 1, 0]

TABLE I: Lattice vectors for the different kind of cubic Bravais lattices.

	N_1	N_2	N_3
sc	$N^{1/3}$	$N^{1/3}$	$N^{1/3}$
bcc	$(\frac{N}{2})^{1/3}$	$(\frac{N}{2})^{1/3}$	$2(\frac{N}{2})^{1/3}$
fcc	$(\frac{N}{4})^{1/3}$	$(\frac{N}{4})^{1/3}$	$4(\frac{N}{4})^{1/3}$

TABLE II: Associated number particles with the lattices vectors listed in Table I for the different kind of cubic Bravais lattices.

in each direction (compatible with the total number of particles). We give in Table I a set of primitive lattice vectors and in Table II the particle number associated with them (for a total of N particles) for a sc, bcc and fcc lattices which fulfill the above requirements.

B. Generation of vectors in reciprocal space in the FBZ

Given the primitive lattice vectors \mathbf{a}_i , the primitive vectors in reciprocal space are univocally defined by Eq. (13). The basis we have used to generate the lattices is given in Table I and the corresponding primitive reciprocal vectors are listed in Table III. The reciprocal vectors are generated using Eq. (12) where m_i are the same integers as the ones used to generate the \mathbf{R} vectors, i.e.,

$$m_i \in [0, N_i - 1] \cap \mathbb{Z}. \quad (30)$$

It is necessary, in order to use FFT techniques, to generate the reciprocal vectors in this way, as we will see in section III C.

However, all the \mathbf{k} vectors used in the computation of the evolution of the particle position must lie in the FBZ (see section II B) but, in general, those generated using Eqs. (12) and (30) do not. We can translate the reciprocal vectors into the FBZ using the transformation

	\mathbf{b}_1	\mathbf{b}_2	\mathbf{b}_3
sc	$2\pi[1, 0, 0]$	$2\pi[0, 1, 0]$	$2\pi[0, 0, 1]$
bcc	$2\pi[1, 0, -1]$	$2\pi[0, 1, -1]$	$4\pi[0, 0, 1]$
fcc	$4\pi[-1, 0, 1]$	$4\pi[1, 0, 0]$	$2\pi[1, 1, -1]$

TABLE III: Reciprocal vectors for the different lattices.

sc	bcc	fcc
$\frac{\pi}{\ell} [\pm 1, 0, 0]$	$\frac{\pi}{\ell} [0, \pm 1, \pm 1]$	$\frac{2\pi}{\ell} [\pm 1, 0, 0]$
$\frac{\pi}{\ell} [0, \pm 1, 0]$	$\frac{\pi}{\ell} [\pm 1, 0, \pm 1]$	$\frac{2\pi}{\ell} [0, \pm 1, 0]$
$\frac{\pi}{\ell} [0, 0, \pm 1]$	$\frac{\pi}{\ell} [\pm 1, \pm 1, 0]$	$\frac{2\pi}{\ell} [0, 0, \pm 1]$
		$\frac{\pi}{\ell} [\pm 1, \pm 1, \pm 1]$
2 + 2 + 2 vectors	4 + 4 + 4 vectors	2 + 2 + 2 + 8 vectors

TABLE IV: Normal vectors which define the FBZ of the bcc and fcc lattices.

which leads Eq. (18) invariant

$$\mathbf{k} \longrightarrow \mathbf{k} + \sum_{i=1}^3 m'_i \mathbf{b}_i, \quad (31)$$

where m'_i are some appropriate integers.

One can obtain a complete set of N \mathbf{k} vectors which are in the FBZ, in the following way: compute a set of candidate vectors to lie in the FBZ with Eqs. (12) and (31). To select those which are in the FBZ, it is not efficient to consider the N vectors with smaller modulus because it is an $\mathcal{O}(N^2)$ operation. The computation time for this can be prohibitive for large N . It is much better to construct geometrically the shape of the FBZ by considering some point of the reciprocal space (namely $\mathbf{b} = \mathbf{0}$) and then drawing the perpendicular bisector planes of the translation vectors from the chosen center to the nearest sites of the reciprocal lattice. In Table IV, we give the normal vector of this plane, with modulus equal to their closest distance to the center $\mathbf{k} = \mathbf{0}$. The FBZ of the sc lattice is a cube of side $2\pi/\ell$, the one of the bcc lattice a rhombic dodecahedron and the one of the fcc lattice a cuboctahedron. Then, we select the \mathbf{k} vectors which are enclosed between these planes. This is an essentially $\mathcal{O}(N)$ operation.

C. Fast Fourier Transform

In this section, we will carry out the FFT of some quantity defined on the lattice as, e.g., the dynamical matrix

$$\tilde{\mathcal{D}}(\mathbf{k}) = \sum_{\mathbf{R}} \mathcal{D}(\mathbf{R}) e^{i\mathbf{k}\cdot\mathbf{R}}, \quad (32)$$

where \mathbf{R} is restricted to the simulation box. Equation (32) involves an $\mathcal{O}(N^2)$ operations (an N -term sum for each of the N \mathbf{k} vectors). However, using the so-called *Fast Fourier Transform* (FFT) technique, it is possible to reduce the number of operations — exploiting the symmetries of the FT — to only $N \ln_2 N$ operations. We give a brief summary of how the FFT works in App. C. By using it, we can speed-up greatly the computation of the FTs of the dynamical matrix and the displacement field.

Using Eqs. (1), (12) and (13) we can write Eq. (32) as

$$\tilde{\mathcal{D}}_{\mathbf{m}} = \sum_{\mathbf{n}} \mathcal{D}_{\mathbf{n}} \exp \left[2\pi i \left(\frac{n_1 m_1}{N_1} + \frac{n_2 m_2}{N_2} + \frac{n_3 m_3}{N_3} \right) \right], \quad (33)$$

where the indices \mathbf{n} and \mathbf{m} labels the \mathbf{R} and \mathbf{k} vectors respectively. These are the same triplets of integers which have been used in Eqs. (1) and (12) respectively. Note that Eq. (33) is a three-dimensional FT, i.e., three embedded one-dimensional FT as the one of Eq. (C1), with the same running of indices [see Eqs. (2) and (30)]. It is then straightforward to compute the FT (33) using any standard FFT routine. Note that each \mathbf{R} vector should be associated in Eq. (33) with the indices $[n_1, n_2, n_3]$ with which it has been generated using Eq. (1), and not those that would correspond to their actual position in the cubic box after being applied the transformation (29). The same observation holds for the \mathbf{k} vectors, whose indices correspond to those used generating them with Eq. (12).

There exists a great number of publicly available very competitive FFT routines. We have used the *Fastest Fourier Transform in the West* (FFTW) [17], since it can be used for any number of particles (and not only powers of two).

D. Spectrum of eigenvalues of an sc, bcc and fcc lattices

As an application of these techniques, we show in Fig. 1 the spectrum of eigenvalues corresponding to a sc, bcc and fcc lattice. We use a cubic box and $N_{sc} = 64$ for the sc lattice. For a comparison with the other lattices, we need $N_{bcc} = 51$ and $N_{fcc} = 40$. The three lattice presents the same branch structure (for further discussion see [10]): (i) an *optical branch*, with eigenvalues $\varepsilon(\mathbf{k}\ell \rightarrow \mathbf{0}) = 1$ and eigenvector polarized parallel to \mathbf{k} (in the same limit) and (ii) two *acoustic branches* with normalized eigenvalues $\varepsilon(\mathbf{k}\ell \rightarrow \mathbf{0}) = 0$ and polarized in the plane transverse to \mathbf{k} (in the same limit). We also see that, as anticipated in [10], the spectrum of the bcc and fcc lattices does not present negative nor eigenvalues with $\varepsilon(\mathbf{k}) > 1$.

IV. DISCRETENESS EFFECTS IN A BCC, FCC AND SC LATTICE

In this section, we will apply the method described above to compare the discreteness effects when using different lattices to set-up the IC, i.e., different discretizations of the same initial density field. To do that, we compare FLT with PLT for the three lattices considered. We will study two different effects: the change in the amplification of the PS and the breaking of isotropy. A more detailed study of discreteness effects in the linear regime for a sc lattice can be found in [12].

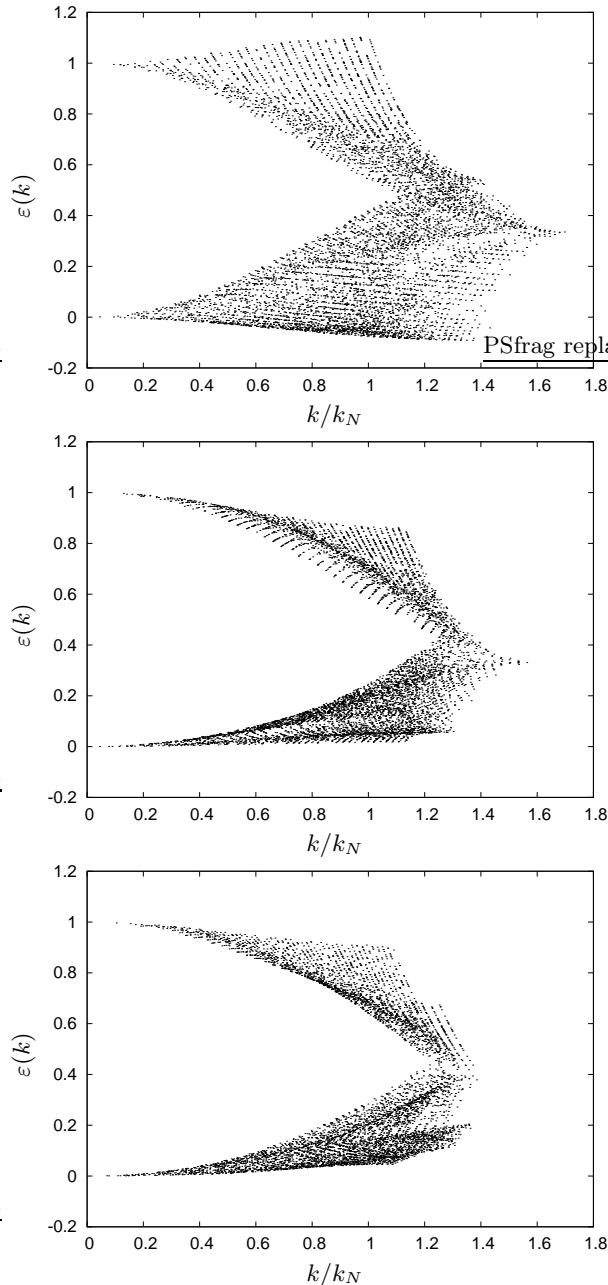


FIG. 1: Normalized spectrum of eigenvalues of (from top to bottom) a sc, bcc and fcc in function of the wavevector normalized to the Nyquist frequency of the sc lattice defined in Eq. (14). We have performed a sampling taking 1% of the points.

In the fluid limit the evolution of the PS is given by the well-known FLT (e.g.[1, 10]):

$$P^{\text{fluid}}(k, t) = a^2(t)P(k, t_0) \quad (34)$$

[we consider an initial PS which is statistically isotropic and we have used that $a(t_0) = 1$, see Eq. (B2)]. The evolution using PLT, is given by Eqs. (26) and (27). We set up the IC by using the ZA approximation.

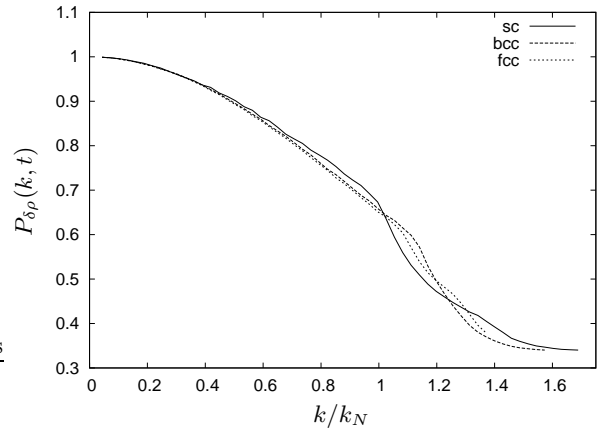


FIG. 2: Amplification of the PS averaged over bins normalized to the fluid (FLT) amplification. The wavevectors have been normalized to the Nyquist frequency of the sc lattice (see the text for more details).

To characterize the effect of the discreteness in the amplification of the PS we define the quantity

$$P_{\delta\rho}(\mathbf{k}, t) = \frac{P(\mathbf{k}, t)}{P^{\text{fluid}}(k, t)}, \quad (35)$$

which is the amplification of the PS calculated with PLT normalized by FLT. In Fig. 2 we show the amplification of the PS at $a(t) = 5$ predicted by PLT, normalized to the fluid amplification. We have averaged over 60 bins centered in $|\mathbf{k}|$ with amplitude $|\mathbf{k}| \pm |\Delta\mathbf{k}|$ with $|\Delta\mathbf{k}| \approx 0.92$. We see that the evolution of the sc lattice is slightly closer to the fluid one ($A_P^2(\mathbf{k}, t)/a(t)^2 = 1$) for $k \lesssim k_N$ than the bcc and fcc lattices. This is not surprising, looking at the form of the spectrum of eigenvalues of the different lattices shown in Fig. 1. The amplification of *each single mode* for $k \ll k_N$ of the PS is related essentially with the shape of the *optical branch* of the spectrum of eigenvalues. There are some eigenvalues in the sc lattice with $\varepsilon(\mathbf{k}) > 1$ which compensate, averaging over bins of same $|\mathbf{k}|$, the largest part of eigenvalues with $\varepsilon(\mathbf{k}) < 1$. However, for $k \gtrsim k_N$, the evolution of the sc lattice is farther than the other two from the fluid evolution. In fact, the modes with $\varepsilon(\mathbf{k}) > 1$ do not exist anymore for $k > k_N$. Therefore, looking at the amplification of the PS, we can say that the sc lattice is slightly closer to the fluid evolution for $k \lesssim k_N$. However, as we will see below, the *anisotropy* introduced by the sc lattice is much larger than the one introduced by the bcc or fcc lattice.

Let us consider the *normalized dispersion* of the amplification of the PS, defined as in [12]

$$\Delta P_{\delta\rho}(k, t) = \left(\frac{\overline{P_{\delta\rho}^2}(k, t) - \overline{P_{\delta\rho}}^2(k, t)}{\overline{P_{\delta\rho}}^2(k, t)} \right)^{1/2} \quad (36)$$

where the average, of any function $X(\mathbf{k}, t)$ on the recip-

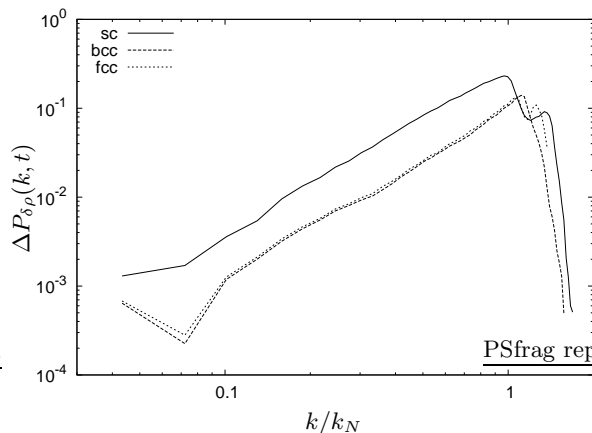


FIG. 3: Normalized dispersion of the PS amplification $\Delta P_{\delta\rho}(k, t)$ averaged over bins of the same modulus of \mathbf{k} .

rocal lattice, is defined as

$$\bar{X}(k, t) = \frac{1}{N_k} \sum_{\mathbf{k}, |\mathbf{k}|=k} X(\mathbf{k}, t), \quad (37)$$

N_k being the number of eigenmodes at a given k . This quantity gives a measure of the anisotropy of the PS amplification. In a system which respects the isotropy of a fluid, the amplification of plane waves with the same corresponding wavevector, but different direction, should be the same. In Fig. 3 we show that the sc presents a dispersion which is about an order of magnitude larger than the one of the bcc or fcc, which is very similar. The behavior of the dispersion $\Delta P_{\delta\rho}(k, t) \propto k^4$ as predicted by PLT because the eigenvalues, for $|\mathbf{k}| \lesssim k_N$, goes as $\varepsilon(\mathbf{k}) \simeq 1 - \alpha(\hat{\mathbf{k}})k^2/k_N^2$, where $\alpha(\hat{\mathbf{k}})$ is a function which depends on the particular lattice (for more details see [10]).

Another method to quantify explicitly the breaking of isotropy consists in measuring the deviation of the eigenvalues corresponding to the *optical* branch with the polarization of them in the fluid limit in the direction $\hat{\mathbf{k}}$ (see [10, 12]). We can quantify it using the expression:

$$\tilde{D}_{\text{aniso}}(\mathbf{k}, t) = \frac{|\tilde{\mathbf{u}}(\mathbf{k}, t) - \hat{\mathbf{k}} \cdot \tilde{\mathbf{u}}(\mathbf{k}, t)\hat{\mathbf{k}}|^2}{|\hat{\mathbf{k}} \cdot \tilde{\mathbf{u}}(\mathbf{k}, t)|^2}. \quad (38)$$

In the infinite realizations limit, assuming that the IC have been set-up using the ZA [i.e. the expression (25) holds], using Eq. (28) we have:

$$\langle \tilde{D}_{\text{aniso}}(\mathbf{k}, t) \rangle_{ZA} = \left| \frac{\mathcal{A}_{\mu\nu}\mathcal{A}_{\mu\sigma}\hat{\mathbf{k}}_\nu\hat{\mathbf{k}}_\sigma}{(\mathcal{A}_{\mu\nu}\hat{\mathbf{k}}_\mu\hat{\mathbf{k}}_\nu)^2} \right|. \quad (39)$$

For sufficiently long times (i.e. some dynamical times $\tau_{\text{dyn}} = 1/\sqrt{4\pi G\rho_0}$) the expression (39) is independent on how the IC have been set-up and on the cosmological model. It depends only on the eigenvectors, i.e., the particular lattice:

$$\langle \tilde{D}_{\text{aniso}}(\mathbf{k}, t \gg t_0) \rangle \approx \frac{1}{(\hat{\mathbf{e}}_1(\mathbf{k}) \cdot \hat{\mathbf{k}})^2}, \quad (40)$$

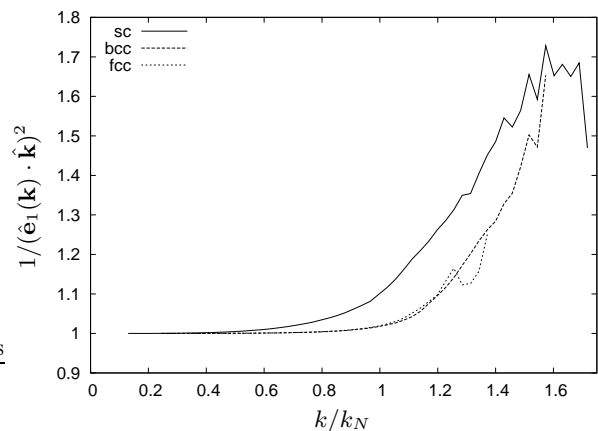


FIG. 4: Deviation of the polarization of the eigenvectors from the fluid limit $\langle \tilde{D}_{\text{aniso}}(\mathbf{k}, t \gg t_0) \rangle$.

where $\hat{\mathbf{e}}_1(\mathbf{k})$ is the eigenvector corresponding to the optical branch, i.e., the one with maximal associated eigenvalue. We plot this quantity in Fig. 4. Once again, we see that the bcc and fcc lattices are very similar, while the breaking of isotropy of the sc lattice is much larger.

V. CONCLUSIONS AND PERSPECTIVES

In this technical paper we have explained step-by-step how to apply the Particle Linear Theory to a cubic Bravais lattice (sc, bcc and fcc lattices) in a *cubic* simulation box. We use FFT techniques to speed-up the numerical computations, which permits to compute the evolution of the position of a large number of particles in a small computation time even with modest computer resources. We have illustrated the method computing the discreteness effects — in the linear regime — resulting from the evolution of continuous density field discretized using a perturbed bcc, fcc and sc lattice. Attending to the tests we have performed, the bcc and fcc discretizations present less discreteness effects — in this regime — than the sc one, presenting small differences between them. They might be therefore better choices to set-up the IC in cosmological N-body simulations.

As pointed-out in the introduction, an important motivation of this work — and the reason for which we have actually developed it — is the study of the discreteness effects in the highly-non linear (non-perturbative) regime. A way to estimate the discreteness effects in this regime consists in running a set of simulations set-up with different Bravais cubic lattices [13]. They lead to results which differ between them in a few per cent in the PS. From the IC and the final measured PS, a lot ingredients enter in the game: the parameters of numerical integration — strategy and accuracy in the computation of the force, smoothing, time-step —, finite-size effects, noise of the estimator, statistical fluctuations... It is important to have an analytic tool to check that the differences

observed in the simulations corresponds actually to discreteness effects. The PLT plays this role in the linear regime of gravitational clustering (i.e. “small” k in the PS), which strongly suggests that the effects observed are actually discreteness ones in the *whole* range of k .

We have described the method for an EdS universe. It is possible to generalize the treatment for a flat background model with cosmological constant — which is the currently most favored one —, without much extra-numerical cost. An implementation of the PLT for this kind of background model will be presented in a forthcoming paper.

We have considered only *cubic* Bravais lattices. The method can be also applied to *any* Bravais lattice with the caveat that, in some cases, the simulations box could not always be a cube, i.e., the vectors \mathbf{R} might not be translated into a cube using the transformation (29).

Acknowledgments

I thank A. Gabrielli, S. Gaudio, J. Lorenzana and M. Joyce for many helpful discussions and comments.

APPENDIX A: EWALD SUM OF THE DYNAMICAL MATRIX

The Ewald sum for the dynamical matrix is:

$$\mathcal{D}(\mathbf{R}) = \mathcal{D}^{(r)}(\mathbf{R}) + \mathcal{D}^{(k)}(\mathbf{R}) \quad (\text{A1})$$

with

$$\begin{aligned} \mathcal{D}_{\mu\nu}^{(r)}(\mathbf{R} \neq \mathbf{0}) &= -Gm \sum_{\mathbf{n}} \left[\frac{(\mathbf{R} - \mathbf{n} \cdot \mathbf{A})_{\mu} (\mathbf{R} - \mathbf{n} \cdot \mathbf{A})_{\nu}}{|\mathbf{R} - \mathbf{n} \cdot \mathbf{A}|^2} \right] \frac{4\alpha^3}{\sqrt{\pi}} \exp(-\alpha^2 |\mathbf{R} - \mathbf{n} \cdot \mathbf{A}|^2) \\ &+ Gm \sum_{\mathbf{n}} \left[\frac{\delta_{\mu\nu}}{|\mathbf{R} - \mathbf{n} \cdot \mathbf{A}|^3} - 3 \frac{(\mathbf{R} - \mathbf{n} \cdot \mathbf{A})_{\mu} (\mathbf{R} - \mathbf{n} \cdot \mathbf{A})_{\nu}}{|\mathbf{R} - \mathbf{n} \cdot \mathbf{A}|^5} \right] \left[\text{erfc}(\alpha |\mathbf{R} - \mathbf{n} \cdot \mathbf{A}|) + \frac{2\alpha}{\sqrt{\pi}} \exp(-\alpha^2 |\mathbf{R} - \mathbf{n} \cdot \mathbf{A}|^2) |\mathbf{R} - \mathbf{n} \cdot \mathbf{A}| \right] \end{aligned} \quad (\text{A2})$$

and

$$\mathcal{D}_{\mu\nu}^{(k)}(\mathbf{R}) = \frac{4\pi Gm}{V_B} \sum_{\mathbf{k} \neq \mathbf{0}} \frac{1}{|\mathbf{k}|^2} \exp\left(-\frac{|\mathbf{k}|^2}{4\alpha^2}\right) \cos(\mathbf{k} \cdot \mathbf{R}) k_{\mu} k_{\nu}. \quad (\text{A3})$$

Note that the sum in Eq. (A3) is over *all* Fourier space and not only in the FBZ. The $\mathbf{R} = \mathbf{0}$ term is

$$\mathcal{D}(\mathbf{R} = \mathbf{0}) = - \sum_{\mathbf{R} \neq \mathbf{0}, \mathbf{n}} \mathcal{D}(\mathbf{R} + \mathbf{n} \cdot \mathbf{A}). \quad (\text{A4})$$

In order to sum over a minimal number of vectors in real and Fourier space we take $\alpha \approx 2.067$.

APPENDIX B: SOLUTION OF THE MODE EQUATIONS

We choose the solutions $U_n(\mathbf{k}, t)$ and $V_n(\mathbf{k}, t)$ of the mode equation (21), without any loss of generality, satisfying

$$U_n(\mathbf{k}, t_0) = 1, \quad \dot{U}_n(\mathbf{k}, t_0) = 0, \quad (\text{B1a})$$

$$V_n(\mathbf{k}, t_0) = 0, \quad \dot{V}_n(\mathbf{k}, t_0) = 1. \quad (\text{B1b})$$

For an EdS universe the scale factor is [1]:

$$a(t) = \left(\frac{t}{t_0}\right)^{2/3}. \quad (\text{B2})$$

In this particular case the functions $U_n(\mathbf{k}, t)$ and $V_n(\mathbf{k}, t)$ can be calculated analytically and are:

$$U_n(\mathbf{k}, t) = \tilde{\alpha}(\mathbf{k}) \left[\alpha_n^+(\mathbf{k}) \left(\frac{t}{t_0}\right)^{\alpha_n^-(\mathbf{k})} + \alpha_n^-(\mathbf{k}) \left(\frac{t}{t_0}\right)^{-\alpha_n^+(\mathbf{k})} \right] \quad (\text{B3a})$$

$$V_n(\mathbf{k}, t) = \tilde{\alpha}(\mathbf{k}) t_0 \left[\left(\frac{t}{t_0}\right)^{\alpha_n^-(\mathbf{k})} - \left(\frac{t}{t_0}\right)^{-\alpha_n^+(\mathbf{k})} \right] \quad (\text{B3b})$$

where

$$\tilde{\alpha}(\mathbf{k}) = \frac{1}{\alpha_n^-(\mathbf{k}) + \alpha_n^+(\mathbf{k})} \quad (\text{B4})$$

and

$$\alpha_n^-(\mathbf{k}) = \frac{1}{6} \left[\sqrt{1 + 24\varepsilon_n(\mathbf{k})} - 1 \right], \quad (\text{B5a})$$

$$\alpha_n^+(\mathbf{k}) = \frac{1}{6} \left[\sqrt{1 + 24\varepsilon_n(\mathbf{k})} + 1 \right]. \quad (\text{B5b})$$

If $\varepsilon_n(\mathbf{k}) > 0$ the solution presents a power-law amplification mode and a power-law decaying mode. If $-1/24 < \varepsilon_n(\mathbf{k}) < 0$, there are two decaying modes. Finally, if $\varepsilon_n(\mathbf{k}) \leq -1/24$, the solution is oscillatory and

can be written as

$$U_n(\mathbf{k}, t) = \left(\frac{t}{t_0}\right)^{-\frac{1}{6}} \cos \left[\gamma_n(\mathbf{k}) \ln \left(\frac{t}{t_0}\right) \right] + \frac{1}{6\gamma_n(\mathbf{k})} \left(\frac{t}{t_0}\right)^{-\frac{1}{6}} \sin \left[\gamma_n(\mathbf{k}) \ln \left(\frac{t}{t_0}\right) \right], \quad (\text{B6a})$$

$$V_n(\mathbf{k}, t) = \frac{t_0}{\gamma_n(\mathbf{k})} \left(\frac{t}{t_0}\right)^{-\frac{1}{6}} \sin \left[\gamma_n(\mathbf{k}) \ln \left(\frac{t}{t_0}\right) \right] \quad (\text{B6b})$$

where

$$\gamma_n(\mathbf{k}) = \frac{1}{6} \sqrt{|24\varepsilon_n(\mathbf{k}) + 1|}. \quad (\text{B7})$$

The evolution of the displacement field from any initial state $\mathbf{u}(\mathbf{R}, t_0)$ is then given by the transformation

$$\mathbf{u}(\mathbf{R}, t) = \frac{1}{N} \sum_{\mathbf{k}} \left[\mathcal{P}(\mathbf{k}, t) \tilde{\mathbf{u}}(\mathbf{k}, t_0) + \mathcal{Q}(\mathbf{k}, t) \dot{\tilde{\mathbf{u}}}(\mathbf{k}, t_0) \right] e^{i\mathbf{k}\cdot\mathbf{R}} \quad (\text{B8})$$

where the matrix elements of the ‘‘evolution operators’’ \mathcal{P} and \mathcal{Q} are

$$\mathcal{P}_{\mu\nu}(\mathbf{k}, t) = \sum_{n=1}^3 U_n(\mathbf{k}, t) (\hat{\mathbf{e}}_n(\mathbf{k}))_{\mu} (\hat{\mathbf{e}}_n(\mathbf{k}))_{\nu}, \quad (\text{B9a})$$

$$\mathcal{Q}_{\mu\nu}(\mathbf{k}, t) = \sum_{n=1}^3 V_n(\mathbf{k}, t) (\hat{\mathbf{e}}_n(\mathbf{k}))_{\mu} (\hat{\mathbf{e}}_n(\mathbf{k}))_{\nu}. \quad (\text{B9b})$$

APPENDIX C: A BRIEF SUMMARY OF THE FFT TECHNIQUE

Let us consider for sake of simplicity the one-dimensional FT \tilde{f} of the function f :

$$\tilde{f}_k = \sum_{j=0}^{N-1} e^{i2\pi jk/N} f_j. \quad (\text{C1})$$

Because of the symmetries of the FT it is possible to divide the sum (C1) (with N terms) into two sums with $N/2$ terms (this is called the *Danielson-Lanczos* lemma):

$$\tilde{f}_k = \sum_{j=0}^{N/2-1} e^{i2\pi jk/(N/2)} f_{2j} + e^{i2\pi k/N} \sum_{j=0}^{N/2-1} e^{i2\pi jk/(N/2)} f_{2j+1}, \quad (\text{C2})$$

i.e., an ‘‘even’’ and ‘‘odd’’ term. Therefore, at this stage, it is possible to compute the even and odd sums at the same time, and then sum the result to obtain the desired FT. It involves a total of $N \times (N/2) + 1$ operations, instead of N^2 . For a number of particles which is a power of two, we can perform recursively the division (C2) $\ln_2 N$ times. Therefore the computation of the N terms \tilde{f}_k involves only $N \ln_2 N$ operations. This is called the *Cooley-Tukey FFT algorithm*. It exist other algorithms (which we will not describe here), which can use *any* number N of particles (and not only a power of two).

-
- [1] P. J. E. Peebles, *The Large-Scale structure of the Universe* (Princeton University Press, Princeton, 1980).
- [2] A. L. Melott, *Comments Astrophys.* **15**, 1 (1990)
- [3] B. Kuhlman, A. L. Melott and S. F. Shandarin, *Astrophys. J.* **470**, L41 (1996)
- [4] A. L. Melott, S. F. Shandarin, R. J. Splinter and Y. Suto, *Astrophys. J.* **479**, L79 (1997)
- [5] R. J. Splinter, A. L. Melott, S. F. Shandarin and Y. Suto, *Astrophys. J.* **497**, 38 (1998)
- [6] K. Heitmann, P. M. Ricker, M. S. Warren and S. Habib, *ApJS* **160**, 28 (2005), (2004), [astro-ph/0411795](#).
- [7] J. Diemand, B. Moore J. Stadel and S. Kazantzidis, *Mon. Not. Roy. Astron. Soc.* **348**, 977 (2004), [astro-ph/0304549](#).
- [8] C. Power et al., *Mon. Not. Roy. Astron. Soc.* **338**, 14 (2003), [astro-ph/0201544](#).
- [9] M. Joyce and B. Marcos, *Phys. Rev. D* **75**, 063516 (2007), [astro-ph/0410451](#).
- [10] B. Marcos, T. Baertschiger, M. Joyce, A. Gabrielli and F. Sylos Labini, *Phys. Rev.* **D73**, 103507 (2006), [astro-ph/0601479](#).
- [11] M. Joyce, B. Marcos, A. Gabrielli, T. Baertschiger and F. Sylos Labini, *Phys. Rev. Lett.* **95**, 011304 (2005), [astro-ph/0504213](#).
- [12] M. Joyce and B. Marcos, *Phys. Rev. D* **76**, 103505 (2007), [arXiv:0704.3697v1](#).
- [13] M. Joyce, B. Marcos and T. Baertschiger, in preparation (2008).
- [14] R. W. Hockney and J. W. Eastwood, *Computer simulation using particles* (Taylor & Francis, 1998).
- [15] D. Pines, *Elementary excitations in solids* (Benjamin, 1963).
- [16] A. Gabrielli, *Phys. Rev. E* **70**, 066131 (2004).
- [17] <http://www.fftw.org/>.